the possibility of revaccination has not been considered; if vaccines have low efficacy as a result of the waning of vaccine-induced immunity, then it may be very simple to increase vaccine efficacy by developing an appropriate revaccination schedule (*1*). Obviously, the development of an optimal vaccination campaign for HIV eradication may include the targeting of high-risk subgroups within the gay community and may include revaccination. The development of such optimal vaccination programs for HIV eradication therefore requires further theoretical exploration.

The results of our analysis suggest that extremely effective vaccines will have to be applied at high coverage levels to achieve HIV eradication (*10*). The available data indicate that it may be very difficult to achieve the necessary high participation rates unless highly efficacious vaccines are developed. The results demonstrate that risk behavior change and mass vaccination campaigns have to be considered together, and that it is extremely unlikely that vaccines will be able to eradicate HIV in San Francisco unless they are combined with considerable reductions in risk behaviors. If one of the consequences of a mass vaccination campaign is an increase in the level of risk behavior, the results indicate that it may become impossible to eradicate HIV. Although we wish to stress that if HIV eradication proves to be impossible, prophylactic vaccines (as we have shown elsewhere) could significantly reduce the HIV epidemic (*1*). However, the potential consequences of HIV mass vaccination campaigns need to be evaluated carefully, because (as we have shown in this analysis) such campaigns could result in a perverse outcome by increasing the severity of the epidemic. Therefore, the results illustrate that it is essential that efficacious prophylactic vaccines and efficacious behavioral intervention strategies be developed concurrently. A number of HIV prophylactic vaccines have already passed through phase I and phase II clinical trials. A recent decision has been made to delay phase III trials. This decision has the beneficial effect of allowing more time for the development of a quantitative theoretical framework for assessing the potential impact of prophylactic vaccines. We suggest that the developing theoretical framework should now be used in guiding the design of the phase III clinical trials, as well as in guiding the design of future mass vaccination campaigns.

REFERENCES AND NOTES

1. A. R. McLean and S. M. Blower, *Proc. R. Soc. London Ser. B* **253**, 9 (1993).
2. P. G. Smith, L. C. Rodrigues, P. E. M. Fine, *Int. J. Epidemiol.* **13**, 87 (1984).
3. I. M. Longini, M. E. Halloran, M. Haber, R. T. Chen, *Stat. Med.* **12**, 249 (1993).
4. M. E. Halloran, M. Haber, I. M. Longini, *Am. J. Epidemiol.* **136**, 328 (1992).
5. G. Macdonald, *Trop. Dis. Bull.* **49**, 813 (1952).
6. R. M. Anderson and R. M. May, *Infectious Diseases of Humans* (Oxford Univ. Press, London, 1991).
7. D. H. Osmond *et al.*, *Am. J. Public Health*, in press.
8. We obtained these estimates by using data from the SFYMHS and the equation $R_0 = \beta cD$ (*6*) (where β is the average transmission efficiency of HIV per sexual partnership, c is the average number of receptive anal sex partners experienced per unit time, and D is the average duration of infectiousness). To obtain the lower bound estimate we used risk behavior data only from the seronegative respondents, and to obtain the upper bound estimate we used risk behavior data from the entire cohort.
9. Any behavioral changes that affect either the level of condom use (which alters the value of β) or the rate of acquisition of receptive anal sex partners (which alters the value of c) will change the level of the risk behavior (βc). The initial value of βc was calculated from data from SFYMHS seronegative respondents (for the lower bound estimate) and from data from the entire SFYMHS cohort (for the upper bound estimate). In each case (either the upper bound estimate or the lower bound estimate) the initial value of βc was used as a standard and set to 1. We evaluated the risks of changing risk behavior by varying the relative level of the variable βc over the range 0 to 2. For each specific value of βc within this specified range of values we calculated the corresponding value of R_0 ($R_0 = \beta cD$). We then derived (using Eq. 2), for three specific efficacy levels (ϕ = 0.6, 0.8, and 1.0), the critical proportion that needed to be vaccinated in order to eradicate HIV.
10. In this analysis we have not presented any estimates of the number of years that it would take to eradicate HIV in San Francisco; eradication time estimates will be presented in a subsequent publication. The time to the eradication of HIV after a mass vaccination campaign has been initiated will be determined by several factors: the efficacy level of the vaccine, the attained vaccination coverage levels, the mechanism of action of the vaccine (that is, the relative contribution of take, degree, and duration), the incubation period of HIV, the surveillance criterion that is used to define eradication, the initial level of risk behavior, and the stability of risk behavior.
11. These data were collected by asking the respondents the following questions regarding their potential participation in a double-blind phase III vaccine efficacy trial: "Suppose you knew that the vaccine being tested was at least 80% effective—that is, at least 8 out of every 10 people who had received the vaccine would be protected against HIV infection. Would knowing this make you more or less likely to participate in a phase III vaccine trial or wouldn't that make any difference in your willingness to participate?" and "Suppose you knew that the vaccine being tested was somewhere between 40 and 60% effective—that is, between 4 and 6 out of every 10 people who had received the vaccine would be protected against HIV infection. Would knowing this make you more or less likely to participate in a phase III vaccine trial or wouldn't that make any difference in your willingness to participate?"

12. We thank W. Winkelstein Jr., D. Osmond, and J. Wiley for providing access to data from the SFYMHS and for many useful comments. Supported by National Institute on Drug Abuse grant 1R29DA08153 and National Institute of Allergic and Infectious Diseases grant AI33831 (S.M.B.) and by The Royal Society (A.R.M.). We thank the participants of the SFYMHS, D. Peterson, A. Reingold, M. van Oss, N. Freimer, J. Freimer, and D. Freimer.

12 May 1994; accepted 2 August 1994

Degradation of Gα by the N-End Rule Pathway

Kiran Madura* and Alexander Varshavsky†

The N-end rule relates the in vivo half-life of a protein to the identity of its amino-terminal residue. Overexpression of targeting components of the N-end rule pathway in *Saccharomyces cerevisiae* inhibited the growth of haploid but not diploid cells. This ploidy-dependent toxicity was shown to result from enhanced degradation of Gpa1, the α subunit (Gα) of a heterotrimeric guanine nucleotide–binding protein (G protein) that regulates cell differentiation in response to mating pheromones. Sst2, a protein whose absence renders cells hypersensitive to pheromone, was essential for degradation of Gα but not other N-end rule substrates, suggesting the involvement of an indirect, or trans-, targeting mechanism. Gα degradation by the N-end rule pathway adds another regulatory dimension to the multitude of signaling functions mediated by G proteins.

Many regulatory proteins are short-lived in vivo. The metabolic instability of a protein makes possible a rapid adjustment of its concentration or subunit composition through changes in the rates of its synthesis or degradation. The essential determinants of one degradation signal, named the N-degron, are a destabilizing NH_2-terminal residue and an internal lysine residue of a substrate protein (*1–3*). The lysine residue is the site of formation of a multiubiquitin chain, which comprises several covalently linked ubiquitin moieties (*2*, *4*). A set of N-degrons containing different destabilizing residues is manifested as the N-end rule, which relates the in vivo half-life of a protein to the identity of its NH_2-terminal residue (*1*, *2*). Ubiquitin is a 76-residue protein, the conjugation of which to other proteins plays a role in many cellular processes, primarily through routes that involve protein degradation (*4*). The only known physiological substrate of the N-end rule pathway has been the RNA polymerase

Division of Biology, California Institute of Technology, Pasadena, CA 91125, USA.

*Present address: Department of Biochemistry, University of Medicine and Dentistry of New Jersey, R. W. Johnson Medical School, Piscataway, NJ 08854, USA.
†To whom correspondence should be addressed.

of Sindbis virus (*5*). [The N-end rule was discovered with artificial (engineered) protein substrates (*1*, *2*).] We have now identified a second physiological substrate of this pathway: the α subunit of a G protein in *S. cerevisiae*.

The *S. cerevisiae* Ubr1 protein, also termed N-recognin or E3, initiates the targeting of an N-end rule substrate by binding to its NH_2-terminal residue (*2*, *6*). Although *ubr1*Δ mutants are unable to degrade N-end rule substrates, they grow at nearly normal rates and are phenotypically similar to congenic wild-type strains in other respects (*6*). In a search for an informative phenotype linked to the N-end rule pathway, we overexpressed *UBR1* and *UBC2* in yeast from the plasmid pKM1313 (Fig. 1A). The *S. cerevisiae UBC2* gene encodes a 20-kD ubiquitin-conjugating enzyme (*2*, *4*) that is an essential component of the N-end rule pathway and is physically associated with Ubr1 (*7*).

Overexpression of Ubr1 and Ubc2 impaired cell viability: *S. cerevisiae* transformed with pKM1313 grew normally in the presence of glucose, but plating efficiency and growth rate were markedly decreased in the presence of galactose (Fig. 1A). This effect required overexpression of both Ubr1 and Ubc2; the growth of cells that overexpressed either Ubc2 or Ubr1 alone was not impaired (Fig. 1B) (*8*). Both **a**-type and α-type cells (*9*) were sensitive to overexpression of Ubr1 and Ubc2 (Fig. 1A) (*8*). We searched for suppressors of N-end rule toxicity by transforming pKM1313-containing cells with a yeast genomic DNA library. This screen (*10*) yielded a resistance-conferring plasmid, pKM627-2.1, that contained most of the normally repressed *HMLα* locus bearing the *MATα* mating-type cassette (*9*). These and other data (*10*) suggested that the ability of pKM627-2.1 to protect the *MAT***a** strain used in the screen from the toxicity of overexpressed Ubr1 and Ubc2 might result from a pseudodiploid **a**/α state produced in **a**-type cells through expression of the normally silent *HMLα* locus from pKM627-2.1.

This conjecture was confirmed by introducing pKM1313 into diploid **a**/α cells: The growth of transformed cells was unperturbed in the presence of galactose (Fig. 2, A and B). Control experiments showed that Ubr1 and Ubc2 were overexpressed to approximately equal extents in haploid and diploid cells (*8*). The effect of cell ploidy suggested that overexpression of Ubr1 and Ubc2 enhanced the degradation of an N-end rule substrate whose presence, at a certain minimal level, was required for normal growth of haploid but not diploid cells. One candidate for such a substrate was Gα (*11*), a component of the mating response pathway that operates in both **a** and α cell types but is repressed in **a**/α diploids; the latter therefore do not respond to pheromones (*12*). Similar to its homologs in other eukaryotes, the yeast G protein is associated with the inner surface of the plasma membrane and consists of three subunits—α, β, and γ—that are encoded, respectively, by *GPA1*, *STE4*, and *STE18* (*12*, *13*). The binding of a pheromone by a receptor in the plasma membrane results in activation of the receptor-coupled G protein, the α subunit of which exchanges its bound guanosine diphosphate (GDP) for guanosine triphosphate (GTP) and apparently dissociates from the βγ subunits. The active Gβγ complex initiates a cascade of reactions that include growth arrest in the G_1 phase of the cell cycle, induction of specific proteins, and other changes that prepare the cell for mating with a cell of the opposite mating type (*12*, *13*). Hydrolysis of bound GTP by Gα restores the heterotrimeric G protein and thereby inactivates Gβγ. The activated (GTP-containing) Gα participates in adaptation pathways that counteract the mating response; one function of adaptation is to make possible the resumption of cell division in the presence of a pheromone if mating fails to occur (*13*).

If Gα were short-lived, and if its degradation were enhanced by overexpression of Ubr1 and Ubc2, the resulting decrease in the molar ratio of Gα to Gβγ would be expected to impair cell growth by freeing Gβγ to arrest cells in G_1. Because neither Gα nor Gβγ is expressed in diploid (**a**/α) cells (*13*), this model accounted for both

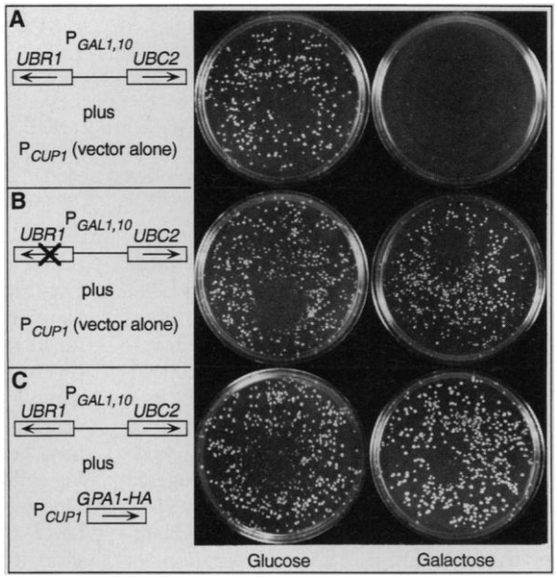

Fig. 1. Toxicity of overexpressed N-end rule pathway components. (**A**) The *S. cerevisiae* strain JD47-13C (*10*) was transformed with pKM1313, a *URA3*-based plasmid containing *UBR1* and *UBC2* under the control of the $P_{GAL1,10}$ promoter (*26*). Transformants were plated on synthetic medium lacking uracil (*23*) and containing glucose or galactose (the latter induces the $P_{GAL1,10}$ promoter). (**B**) As in (A), except cells were transformed with pKM1319, which expressed *UBC2* but not *UBR1* (*26*). (**C**) As in (A), except cells were transformed with both pKM1313 and pKM1362-2, which encoded Gα-HA under the control of the P_{CUP1} promoter (*26*). Cells in (A) and (B) were also transformed with pJDPREdha, a control (vector) counterpart of pKM1362-2.

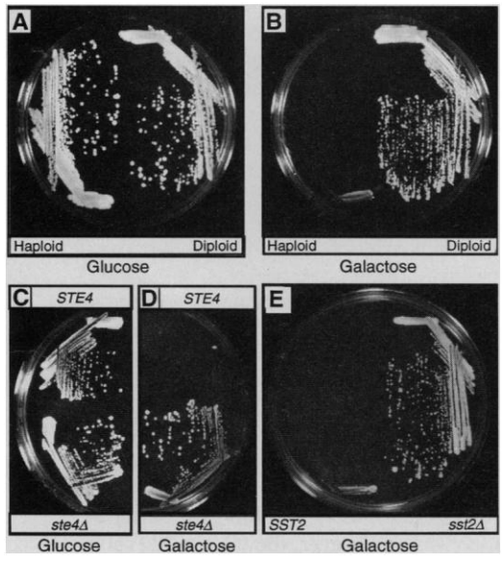

Fig. 2. Toxicity of overexpressed N-end rule pathway components is influenced by cell ploidy and the presence of *STE4* or *SST2*. (**A** and **B**) Haploid (JD47-13C) and diploid (KMD60) *S. cerevisiae* (*27*) were transformed with pKM1313, which expressed *UBR1* and *UBC2* from $P_{GAL1,10}$ (*26*). Transformants were streaked on uracil-lacking synthetic media (*23*) containing glucose (A) or galactose (B). (**C** and **D**) As in (A) and (B), respectively, except that a haploid *ste4*Δ strain and its congenic *STE4* counterpart (*27*) were transformed with pKM1384, a *TRP1*-based counterpart of the *URA3*-based pKM1313 (*26*). (**E**) A haploid *sst2*Δ strain and its congenic *SST2* counterpart KMY901 (*27*) were transformed with pKM1313 (*26*) and streaked on a galactose-containing plate (both strains grew on glucose-containing plates).

the toxicity of overexpressed Ubr1 and Ubc2 and the confinement of toxicity to haploid cells. The model predicted that either overexpression of Gα or elimination of Gβγ should suppress the toxicity. Indeed, haploid cells transformed with pKM1313 and pKM1362-2 (which contains *GPA1* under the control of the P_{CUP1} promoter) continued to grow in the presence of galactose (Fig. 1C). In contrast, the growth of cells transformed with pKM1313 and the vector counterpart of pKM1362-2 was impaired in the presence of galactose (Fig. 1A). We also compared a strain lacking the *STE4*-encoded Gβ subunit (*14*) and a congenic *STE4* strain. The growth of *ste4*Δ cells was unimpaired by overexpression of Ubr1 and Ubc2 (Fig. 2, C and D), in agreement with the model.

To follow the metabolic fate of Gα, we extended its COOH-terminus with a 23-residue sequence containing two copies of the hemagglutinin (HA) epitope (*15*). Cells transformed with pKM1362-2 (which encoded Gα-HA) and pKM1313 were transferred to a galactose-containing medium and incubated with [^{35}S]methionine for 5 min and then incubated for various times in the presence of unlabeled methionine. Proteins were then extracted, immunoprecipitated with antibodies to HA, and fractionated by SDS–polyacrylamide gel electrophoresis (SDS-PAGE). Gα-HA had a half-life of only ~10 min in *S. cerevisiae* overexpressing the N-end rule pathway components (Fig. 3, A and E). In contrast, the half-life of Gα-HA was >10 hours in *ubr1*Δ cells that lacked the N-end rule pathway (Fig. 3, B, D, and E), indicating that the metabolic instability of Gα results from its degradation by this pathway. Gα-HA was a moderately short-lived protein (half-life of ~50 min) in wild-type (*UBR1*) cells that did not overexpress components of the N-end rule pathway (Fig. 3, A, D, and E) (*16*). A decrease in the metabolic stability of Gα in cells overexpressing Ubr1 and Ubc2 was also indicated by a decrease in the amount of ^{35}S associated with Gα-HA immediately after the incubation with [^{35}S]methionine (Fig. 3, A and F); such a change in the labeling intensity of a short-lived protein results at least in part from an alteration in the rate of its degradation during the labeling period (*17*).

Longer fluorographic exposures revealed Gα species larger than the 53-kD Gα-HA (Fig. 4), suggesting that these derivatives of Gα contained a multiubiquitin chain (*2*, *4*). Similar species were also observed with $G\alpha^{451}G\alpha^{472}$-HA, a protein that contained a COOH-terminally truncated, 451-residue Gα linked to the full-length, 472-residue Gα bearing the HA tag (Fig. 4). The large molecular size derivatives of $G\alpha^{451}G\alpha^{472}$-HA were at least as short-lived as the unmodified $G\alpha^{451}G\alpha^{472}$-HA and were more abundant in cells that overexpressed Ubr1 and Ubc2. To verify the presence of ubiquitin in these derivatives of Gα, we transformed cells with a plasmid that encodes a variant of ubiquitin (Myc-Ub) that bears a 13-residue NH_2-terminal extension derived from human c-Myc and is similar to wild-type ubiquitin in its ability to be conjugated to and cleaved off acceptor proteins (*18*). However, because Myc-Ub is ~1.5 kD larger than ubiquitin, the incorporation of Myc-Ub into substrate-linked multiubiquitin chains can be readily detected through a decrease in the electrophoretic mobility of the modified protein (*18*). The derivatives of $G\alpha^{451}G\alpha^{472}$-HA from cells that expressed both wild-type ubiquitin and Myc-Ub indeed migrated more slowly than the analogous species from cells that did not express Myc-Ub (Fig. 4). Similar results were obtained with Gα-HA (*8*). Thus, Gα is ubiquitintated in vivo, as would be expected for a substrate of the N-end rule pathway (*2*).

In yeast and other eukaryotes, the removal of the NH_2-terminal methionine from newly synthesized Gα is followed by the enzymatic myristoylation of the new NH_2-terminal glycine (*11*–*13*). This modification is essential for the function of Gα: Replacement of Gly^2 in *S. cerevisiae* Gα with alanine precludes myristoylation and renders Gα unable to inhibit the activity of Gβγ (*13*). However, the $Gly^2 \rightarrow$Ala substitution did not perturb the degradation of Gα (Fig. 3C), indicating that the myristoylated NH_2-terminus of Gα is not required for its targeting by the N-end rule pathway. Overexpression of the N-end rule pathway components did not result in a significant decrease in substrate specificity of the pathway, because test proteins bearing stabilizing NH_2-terminal residues (*2*) remained long-lived in cells overexpressing Ubr1 and Ubc2 (*8*). In addition, the half-life of a short-lived derivative of the Matα2 repressor [which is targeted by a pathway distinct from the N-end rule pathway (*19*)] was not further decreased in cells overexpressing the N-end rule pathway components (*20*). Gα-βgal, a fusion of Gα and *Escherichia coli* β-galactosidase, was degraded similarly to Gα-HA (Fig. 3) (*8*), indicating that the COOH-terminal HA tag did not contribute to metabolic instability of Gα-HA.

No cleavage products of Gα-HA were observed in metabolic labeling experiments (Fig. 3A), making it unlikely that the targeting of Gα was initiated by a cut that yielded a Gα fragment bearing a destabilizing NH_2-terminal residue. A model in which cleavage was rate-limiting for Gα degradation (which would account for the negligible concentration of a cleavage product) was made unlikely by the absence of changes in the apparent size of Gα-HA from *ubr1*Δ cells (Fig. 3D), in which a cleavage product would be expected to accumulate. Moreover, a Gα-HA tagged at

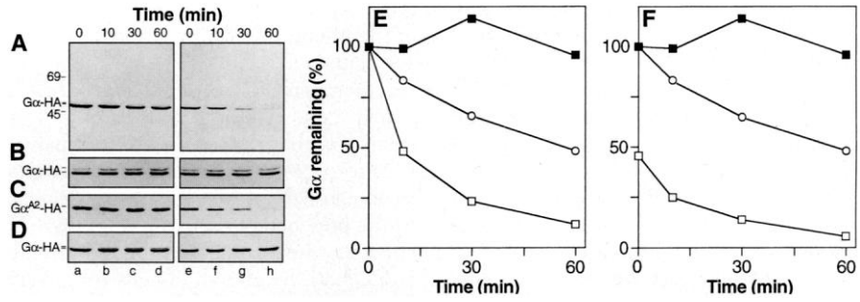

Fig. 3. Metabolic labeling and degradation of Gα in cells containing, lacking, or overexpressing N-end rule pathway components. (**A**) The haploid strain JD47-13C (*10*) transformed with pKM1362-2 (which expressed Gα-HA from P_{CUP1}) and pKM1313 (which expressed *UBR1* and *UBC2* from $P_{GAL1,10}$) (*26*) was grown in synthetic medium containing raffinose (lanes a to d) or galactose (lanes e to h) (*23*). Cells were labeled with [^{35}S]methionine for 5 min at 30°C, and then incubated without label for 0, 10, 30, or 60 min. Samples were subjected to immunoprecipitation with antibodies to the HA epitope, and immunoprecipitates were resolved by SDS-PAGE (*28*). (**B**) As in (A), except with the congenic *ubr1*Δ strain JD55 (transformed with pKM1362-2 and pKM1319) (*26*, *27*), which lacked the N-end rule pathway. (**C**) As in (A), except that instead of pKM1362-2, cells were transformed with pKM1363-2, which encoded $G\alpha^{A2}$-HA (in which the wild-type Gly^2 of Gα-HA was replaced with Ala) (*26*). (**D**) As in (A), except that JD47-13C (*UBR1*) (lanes a to d) or the congenic *ubr1*Δ strain JD55 (lanes e to h) was transformed with only pKM1362-2 and grown in the presence of glucose. A minor band above that of Gα-HA in (A), (B), and (D) corresponds to nonmyristoylated Gα-HA (*13*, *16*, *29*). Positions of 69- and 45-kD molecular mass standards are indicated. (**E**) Electrophoretic patterns obtained with cells grown in galactose were quantified with PhosphorImager (Molecular Dynamics) (*30*). For each of the curves, the amount of ^{35}S in the Gα bands immediately after the labeling period (with the signals form unmodified and myristoylated Gα added together) was taken at 100% (*31*). (■) Gα in *ubr1*Δ *UBC2* cells; (○) Gα in wild-type (*UBR1 UBC2*) cells; and □ Gα in cells overexpressing the N-end rule pathway components. (**F**) As in (E) except that the amount of ^{35}S in Gα immediately after the labeling period in *ubr1*Δ cells was taken at 100%, and ^{35}S values at other points in the three curves were plotted as percentages of that amount (*31*).

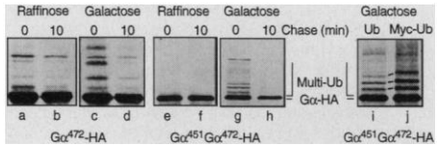

Fig. 4. Multiubiquitination of Gα. (Lanes a and b) the strain JD47-13C (*10*) transformed with pKM1362-2 (which expressed Gα-HA from P_{CUP1}) and pKM1313 (which expressed *UBR1* and *UBC2* from $P_{GAL1,10}$) (*26*) was grown at 30°C in synthetic medium containing raffinose (*23*). Cells were labeled with [^{35}S]methionine for 5 min and then incubated in the absence of label for 0 or 10 min (chase). Samples were subjected to immunoprecipitation with an antibody to the HA epitope, and immunoprecipitates were resolved by SDS-PAGE (*28*). Fluorograms were overexposed approximately tenfold in comparison to those shown in Fig. 3. (Lanes c and d) As in lanes a and b, except that cells were grown in galactose-containing medium, which induced overexpression of Ubr1 and Ubc2. (Lanes e and f) As in lanes a and b, except that cells were transformed with pKM1362-1 (instead of pKM1362-2) (*26*), which encoded $G\alpha^{451}G\alpha^{472}$-HA. (Lanes g and h) As in lanes e and f, except that cells were grown in galactose-containing medium. (Lane i) As in lane g, except from a different experiment. (Lane j) As in lane i, except that cells were also transformed with YEp105, a high–copy number plasmid encoding Myc-Ub under the control of P_{CUP1} (*26*). Half-open brackets indicate ubiquitinated $G\alpha^{451}G\alpha^{472}$-HA. Asterisks between lanes d and e indicate some of the ubiquitinated Gα-HA species. The ~100-kD $G\alpha^{451}G\alpha^{472}$-HA is nearly twice as large as Gα-HA. Ub, ubiquitin.

the NH_2-terminus with the FLAG epitope (*21*) retained this epitope in the course of degradation (*8*), indicating that the NH_2-terminus of Gα is not important in the targeting of the protein by the N-end rule pathway, and that an N-degron of Gα is not produced by an internal cleavage within the Gα polypeptide.

The degradation of N-end rule substrates in *S. cerevisiae* is selectively inhibited by dipeptides that bear destabilizing NH_2-terminal residues and compete with N-end rule substrates for binding to one of the two binding sites in N-recognin (*17*). Specifically, dipeptides bearing a type 1 destabilizing NH_2-terminal residue (*2*) such as Arg inhibit the degradation of N-end rule substrates bearing NH_2-terminal Asn, Gln, Asp, Glu, His, Lys, or Arg. However, the same dipeptides do not inhibit the degradation of otherwise identical substrates bearing any of the type 2 destabilizing NH_2-terminal residues: Phe, Leu, Trp, Tyr, or Ile (*17*). The opposite pattern is observed with dipeptides bearing a type 2 destabilizing NH_2-terminal residue such as Leu (*17*). Degradation of Gα was inhibited by the Leu-Ala dipeptide (added to the medium) but not by Ala-Leu or Arg-Ala (*8*), indicating that an essential step in the targeting of Gα is binding of a type 2 destabilizing NH_2-terminal residue by the type 2 site of N-recognin.

Given these experimental constraints, we considered the possibility that Gα is targeted for degradation in a complex with another protein. The two determinants of an N-degron can residue in different subunits of an oligomeric protein (*2*, *3*). In the case of Gα, this model posits the existence of a protein that binds to Gα and (unlike Gα) bears a destabilizing NH_2-terminal residue, with Gα being targeted in trans. One candidate for this Gα ligand was the Sst2 protein; genetic evidence (*13*, *22*) suggests that Sst2 interacts with Gα. An *sst2Δ* strain, unlike a congenic wild-type (*SST2*) strain, was resistant to overexpression of the N-end rule pathway components (Fig. 2E). Moreover, Gα was metabolically stable in *sst2Δ* cells overexpressing Ubr1 and Ubc2, whereas other (engineered) N-end rule substrates remained short-lived in *sst2Δ* cells (*8*). The discovery that Sst2 is required for Gα degradation by the N-end rule pathway is consistent with the indirect targeting model.

The physiological implications of our results remain to be understood. A *ubr1Δ* mutant, which lacks the N-end rule pathway, was indistinguishable from a congenic wild-type strain in an assay (*23*) that detects the inhibition of cell division by a pheromone (*8*). However, when the response was assessed by measuring the induction of *FUS1*—one of the early response genes (*12*, *13*)—after the addition of α-factor to **a**-type cells, maximal *FUS1* expression was greater in *ubr1Δ* cells than in congenic wild-type (*UBR1*) cells (*8*). Because it is likely that the half-life of Gα is influenced by its functional state (Gα can be GTP- or GDP-bound, covalently modified, or associated with Gβγ, the pheromone receptor, and other Gα ligands), the degradation of Gα in yeast may function either to augment or inhibit cellular responses to a pheromone.

A G_s-type Gα is short-lived in mouse cells (*24*), suggesting that Gα subunits in other organisms may also be degraded by the N-end rule pathway. The activation of mouse Gα shortens its half-life in vivo (*24*), suggesting a regulatory function for the metabolic instability of Gα. Furthermore, the differentiation of rat pheochromocytoma PC12 cells is inhibited by dipeptides bearing destabilizing NH_2-terminal residues (*25*). Our results suggest that dipeptides may suppress cell differentiation through metabolic stabilization of the relevant Gα subunits in PC12 cells.

REFERENCES AND NOTES

1. A. Bachmair, D. Finley, A. Varshavsky, *Science* **234**, 179 (1986); A. Bachmair and A. Varshavsky, *Cell* **56**, 1019 (1989).
2. A. Varshavsky, *Cell* **69**, 725 (1992).
3. E. S. Johnson, D. K. Gonda, A. Varshavsky, *Nature* **346**, 287 (1990).
4. D. Finley and V. Chau, *Annu. Rev. Cell. Biol.* **7**, 25 (1991); M. Rechsteiner, *Cell* **66**, 615 (1991); A. Hershko and A. Ciechanover, *Annu. Rev. Biochem.* **61**, 761 (1992); M. Hochstrasser, *Curr. Opin. Cell Biol.* **4**, 1024 (1992); S. Jentsch, *Annu. Rev. Genet.* **26**, 179 (1992).
5. R. J. deGroot, T. Rümenapf, R. J. Kuhn, E. G. Strauss, J. H. Strauss, *Proc. Natl. Acad. Sci. U.S.A.* **88**, 8967 (1991).
6. B. Bartel, I. Wünning, A. Varshavsky, *EMBO J.* **9**, 3179 (1990).
7. R. J. Dohmen, K. Madura, B. Bartel, A. Varshavsky, *Proc. Natl. Acad. Sci. U.S.A.* **88**, 7351 (1991); K. Madura, R. J. Dohmen, A. Varshavsky, *J. Biol. Chem.* **268**, 12046 (1993).
8. K. Madura and A. Varshavsky, unpublished data.
9. I. Herskowitz, J. Rine, J. Strathern, in *The Molecular and Cellular Biology of the Yeast* Saccharomyces, J. R. Broach, J. R. Pringle, E. W. Jones, Eds. (Cold Spring Harbor Laboratory Press, Cold Spring Harbor, NY, 1992), vol. 2, pp. 583–656.
10. Media and genetic techniques were as described (*6*, *7*, *23*). All media contained 0.1 mM $CuSO_4$. JD47-13C cells (*MAT***a** *his3-Δ200 leu2-2,112 ura3-52 trp1-Δ63 lys2-801*) (*7*) transformed with pKM1313 (*26*) were further transformed with an *S. cerevisiae* genomic DNA library in the high-copy vector YEp13 [K. Nasmyth and S. Reed, *Proc. Natl. Acad. Sci. U.S.A.* **77**, 2119 (1980)]. Transformants were selected on glucose-containing plates, and then replica-plated onto galactose-containing plates to screen for cells resistant to overexpression of the N-end rule pathway components. One resistance-conferring plasmid, pKM627-2.1, contained a DNA insert spanning nucleotides ~9400 to ~13,500 of the sequenced chromosome III [S. G. Oliver *et al.*, *Nature* **357**, 38 (1992)]. This region encompassed most of *HMLα* but lacked a flanking sequence required for the silencing of *HMLα* (*8*).
11. A. G. Gilman, *Annu. Rev. Biochem.* **56**, 615 (1987); H. R. Bourne, D. A. Sanders, F. McCormick, *Nature* **349**, 117 (1991); M. I. Simon, M. P. Strathmann, N. Gautam, *Science* **252**, 802 (1991); L. Birnbaumer, *Annu. Rev. Pharmacol. Toxicol.* **30**, 675 (1990).
12. F. Cross, L. H. Hartwell, C. Jackson, J. B. Konopka, *Annu. Rev. Cell Biol.* **4**, 429 (1988); S. Fields, *Trends Biochem. Sci.* **15**, 270 (1990); L. Marsh, A. M. Neiman, I. Herskowitz, *Annu. Rev. Cell Biol.* **7**, 699 (1991); S. I. Reed, *Curr. Opin. Genet. Dev.* **1**, 391 (1991).
13. J. Kurjan, *Annu. Rev. Genet.* **27**, 147 (1993); G. F. Sprague Jr. and J. W. Thorner, in *The Molecular and Cellular Biology of the Yeast* Saccharomyces, J. R. Broach, J. R. Pringle, E. W. Jones, Eds. (Cold Spring Harbor Laboratory Press, Cold Spring Harbor, NY, 1992), vol. 2, pp. 657–744.
14. M. Whiteway *et al.*, **56**, 467 (1989).
15. J. Field *et al.*, *Mol. Cell. Biol.* **8**, 2159 (1988).
16. H. G. Dohlman, P. Goldsmith, A. M. Spiegel, J. Thorner, *Proc. Natl. Acad. Sci. U.S.A.* **90**, 9688 (1993).
17. R. T. Baker and A. Varshavsky, *ibid.* **88**, 1090 (1991).
18. M. J. Ellison and M. Hochstrasser, *J. Biol. Chem.* **266**, 21150 (1991); M. Hochstrasser, M. J. Ellison, V. Chau, A. Varshavsky, *Proc. Natl. Acad. Sci. U.S.A.* **88**, 4606 (1991).
19. P. Chen, P. Johnson, T. Sommer, S. Jentsch, M. Hochstrasser, *Cell* **74**, 357 (1993).
20. J. Dohmen and A. Varshavsky, unpublished data.
21. B. L. Brizzard, R. G. Chubet, D. L. Vizard, *BioTechniques* **16**, 730 (1994).
22. C. Dietzel and J. Kurjan, *Mol. Cell. Biol.* **7**, 4169 (1987).
23. C. Guthrie and G. R. Fink, Eds., *Guide to Yeast Genetics and Molecular Biology* (Academic Press, New York, 1991).
24. M. J. Levis and H. R. Bourne, *J. Cell Biol.* **119**, 1297 (1992).
25. H. Hondermarck, J. Sy, R. A. Bradshaw, S. M. Arfin, *Biochem. Biophys. Res. Commun.* **189**, 280 (1992).
26. The *UBR1*-containing Bam HI–Pst I fragment from pJD1003 was ligated to YCplac22 cut with the same enzymes (*7*). The resulting plasmid was digested with Sal I and Sph I, and the *UBR1*-containing frag-

ment was ligated to Sal I– and Sph I–digested pKM1167 (which expressed *UBC2* from $P_{GAL1,10}$) (*7*), yielding pKM1308. The latter was cleaved with Pst I and Esp I [removing the adjacent *QCR9* gene (*7*)], treated with T4 DNA polymerase I, and self-ligated, yielding pKM1313. The plasmid pKM1319, which contained a frameshift mutation at codon 172 of *UBR1*, was produced from pKM1313 as described (*7*). *GPA1* (*13*) was isolated from *S. cerevisiae* genomic DNA by the polymerase chain reaction (PCR) [F. M. Ausubel *et al.*, *Current Protocols in Molecular Biology* (Wiley-Interscience, New York, 1992] with primers that allowed the excision of amplified *GPA1* as an ~1.4-kb Eco RI–Kpn I fragment. This fragment was ligated to the Eco RI– and Kpn I–cleaved high-copy plasmid pJDPREdha (provided by J. Dohmen) between its P_{CUP1} promoter and a sequence encoding two tandem HA epitopes (*7*, *15*) [E. S. Johnson, B. Bartel, W. Seufert, A. Varshavsky, *EMBO J.* **11**, 497 (1992)], yielding pKM1362-2. The plasmid pKM1363-2 was constructed similarly to pKM1362-2, except that an amplification primer was designed to convert codon 2 of *GPA1* into an Ala codon. The DNA encoding $G\alpha^{451}G\alpha^{472}$-HA was a by-product of the PCR reaction that yielded Gα-HA DNA. The PCR-derived Eco RI–Kpn I fragment encoding $G\alpha^{451}G\alpha^{472}$-HA was subcloned into pJDPREdha, yielding pKM1362-1. YEp105 (*18*) was provided by E. Johnson.

27. The *S. cerevisiae* strains were JD47-13C (*10*); JD55 (a *ubr1*Δ derivative of JD47-13C) (*7*); KMD60 [the product of a cross between JD47-13C and XS803-2C (*MATα leu2-3,112 ura3-52 his1-7 can*^{r}) (Yeast Strain Collection, University of California, Berkeley)]; W303-1a (*MAT***a** *ade2-1 his3-11 leu2-2, 112 trp1-1 ura3-1 can1-100* [E. Leberer *et al.*, *Mol. Gen. Genet.* **241**, 241 (1993)]; YEL2, a *ste4*Δ*::URA3* derivative of W303-1a (provided by M. Whiteway and J. Dohmen); 29-6, an *sst2*Δ*::URA3* derivative of W303-1a (provided by J. Kurjan); and KMY901, a *Ura*$^-$ derivative of 29-6.
28. Cells were grown at 30°C to an optical density at 600 nm of ~1 in synthetic medium (*23*) containing 3% raffinose instead of glucose. Cultures were diluted by the addition of four volumes of rich (YEP) (*23*) medium containing raffinose or galactose and allowed to grow for 3 hours. Cells from 25-ml cultures were collected by centrifugation, washed with water, and resuspended in 0.4 ml of raffinose or galactose medium lacking methionine. [^{35}S]Methionine (0.2 mCi) (^{35}S-Translabel; ICN) was added, and the suspension was incubated for 5 min at 30°C. The cells were separated by centrifugation and resuspended in otherwise identical medium lacking ^{35}S and containing 10 mM L-methionine, 5 mM L-cysteine, and cycloheximide (0.5 mg/ml). Samples (0.1 ml) were removed either immediately or after 10, 30, or 60 min, added to microfuge tubes with 0.5 g of 0.5-mm glass beads and 0.8 ml of buffer A [1% Triton X-100, 0.15 M NaCl, 5 mM EDTA (Na^+ salt), 50 mM Hepes-NaOH (pH 7.5)] containing protease inhibitors (*6*), and frozen in liquid nitrogen. Thawed samples were agitated for 3 min, with intermittent cooling on ice. The lysates were centrifuged at 12,000*g* for 1 min. Portions of the supernatants containing equal amounts of ^{35}S were incubated with a monoclonal antibody to HA, and then with protein A–Sepharose (Pharmacia). Immunoprecipitated proteins were separated by SDS-PAGE (10% gel and labeled proteins were detected by fluorography (*7*, *17*).
29. D. E. Stone, G. M. Cole, M. B. Lopes, M. Goebl, S. I. Reed, *Genes Dev.* **5**, 1969 (1991).
30. J. W. Tobias, T. E. Shrader, G. Rocap, A. Varshavsky, *Science* **254**, 1374 (1991).
31. Each curve was determined at least twice (five times with cells overexpressing the N-end rule pathway components), in independent experiments, with the results differing by <15% (representative curves are shown in Fig. 3). Because of the non–first order kinetics of Gα degradation, especially in cells overexpressing the N-end rule pathway components, the cited half-lives of Gα were measured between 0 and 10 min after removal of cells from [^{35}S]methionine. Nonexponential degradation is also characteristic of the previously studied (engineered) N-end rule substrates (*1*, *2*, *17*). The effect detected by plotting the data as shown in Fig. 3F was not attributable to a decrease in the rate of Gα-HA synthesis on transfer of cells to galactose, because no such effect was observed with cells that overexpressed Ubc2 alone (*8*).
32. We thank E. Johnson, M. Whiteway, M. Ramezani-Rad, and J. Kurjan for their gifts of plasmids and strains; J. Dohmen for his advice and reagents; and members of our laboratory, especially G. Turner, N. Johnsson, F. Lévy, C. Byrd, M. Ghislain, and J. Johnston, for comments on the manuscript. Supported by grants to A.V. from NIH.

29 April 1994; accepted 26 July 1994

Ras-Dependent Growth Factor Regulation of MEK Kinase in PC12 Cells

Carol A. Lange-Carter* and Gary L. Johnson

Mitogen-activated protein kinases (MAPKs) are rapidly activated in response to stimulation of diverse receptor types. MAPKs are positively regulated by phosphorylation on threonine and tyrosine by MAP kinase or extracellular signal–regulated kinase (ERK) kinases (MEKs). MEK kinase (MEKK) is part of a family of serine-threonine protein kinases that phosphorylate and activate MEKs independently of Raf. MEKK was rapidly and persistently activated in response to stimulation of resting PC12 cells with epidermal growth factor (EGF). Nerve growth factor (NGF) and 12-*O*-tetradecanoylphorbol-13-acetate (TPA) also activated MEKK, although to a lesser degree than did EGF. Activation of MEKK and B-Raf in response to EGF was inhibited by expression of dominant negative N^{17}Ras. Expression of oncogenic Ras resulted in activation of MEKK. Stimulation of synthesis of cyclic adenosine 3′,5′-monophosphate abolished activation of MEKK and B-Raf by EGF, NGF, and TPA. Thus, Ras simultaneously controls the activation of members of the Raf and MEKK families of protein kinases.

The MAP kinase regulatory network is activated as a result of sequential phosphorylation reactions in response to stimulation of cells by growth factors, hormones, or neurotransmitters (*1*, *2*). MAPKs are activated by phosphorylation on specific tyrosine and threonine residues by MAPK (or ERK) kinases (MEKs) (*3*, *4*), of which at least three have been cloned from metazoan species (*5*–*7*). MEKs are in turn regulated by serine-threonine kinases of the Raf family, including c-Raf-1 (*8*, *9*) and B-Raf (*10*, *11*). The mammalian homolog of the yeast protein kinases Byr2 (*Schizosaccharomyces pombe*) and STE11 (*Saccharomyces cerevisiae*), termed MEK kinase (MEKK), also phosphorylates and activates MEKs independently of Raf (*12*). Raf-1 and MEKK phosphorylate the same sites on MEK-1 in vitro, and these sites are phosphorylated in vivo after growth factor stimulation of cells (*13*). Because there are multiple distinct but

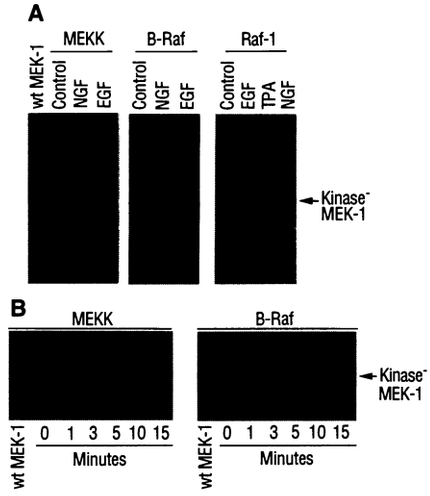

Fig. 1. Activation of MEKK, B-Raf, and Raf-1 by growth factors. (**A**) Phosphorylation of catalytically inactive MEK-1 by immunoprecipitated MEKK, B-Raf, or Raf-1. PC12 cells were incubated in starvation medium [Dulbecco's modified Eagle's medium (DMEM) and 0.1% bovine serum albumin (BSA)] for 18 to 20 hours and left untreated or treated with EGF (30 ng/ml), NGF (100 ng/ml), or TPA (200 nM) for 5 min. MEKK was immunoprecipitated from lysates containing equal amounts of protein with an anitserum to a fusion protein encoding the NH_2-terminal portion of MEKK (*32*). Immunoprecipitations and in vitro kinase assays were performed as described (*33*) with purified recombinant catalytically inactive MEK-1 (150 ng) and 40 μCi of [γ-^{32}P]ATP in a final volume of 20 μl for 25 min at 30°C. B-Raf and Raf-1 were immunoprecipitated from the same untreated and treated PC12 cell lysates described above. Antiserum to a COOH-terminal peptide of B-Raf and anitserum to the 12 COOH-terminal amino acids of Raf-1 (Santa Cruz Biotechnology) were used for the appropriate immunoprecipitations. Equal amounts of MEKK, B-Raf, or Raf-1 were immunoprecipitated from each lysate as demonstrated by immunoblotting (*17*). (**B**) Time course of EGF-stimulated MEKK and B-Raf activation. MEKK or B-Raf was immunoprecipitated from lysates of PC12 cells treated with EGF (30 ng/ml) for 0, 1, 3, 5, 10, 15, or 20 min and incubated with catalytically inactive MEK-1 (150 ng) and [γ-^{32}P]ATP as described for (A).